CIVIL AND ENVIRONMENTAL ENGINEERING REPORTS

E-ISSN 2450-8594

CEER 2024; 34 (4): 0168-0184
DOI: 10.59440/ceer/194260
Original Research Article

APPLICATION OF THE SOUTHWELLTO DETERMINE THE CRITICAL LOAD OF COMPRESSION RODS MADE OF NONLINEAR MATERIALS

Jakub MARCINOWSKI, Mirosław SADOWSKI[1]
University of Zielona Gora, Faculty of Building, Architecture and Environmental Engineering, Poland

A b s t r a c t

Experimental determination of the critical force of a compression bar made of linear material does not pose major problems. The widely used Southwell method is also applicable to bars with cross-sections varying in length. The purpose of the research undertaken was to demonstrate that this method can also be successfully applied to bars made of elastic materials exhibiting nonlinear σ(ε) characteristics. Using analytical relationships for a rod satisfying the assumptions of Euler-Bernoulli theory, F(δ) relationships were derived for a rod with an initial arc imperfection, and Southwell diagrams were constructed on this basis. Nonlinear equilibrium paths F(δ) were also determined numerically using the COSMOS/M program for this purpose. For the pre-assumed different nonlinear characteristics, full confirmation of the validity of the application of the Southwell method for determining the critical force was obtained.

Keywords: bar buckling, critical force, Southwell method, nonlinear material, analytical method, numerical method

1. INTRODUCION

Surprisingly significant advancements in material technology allow for increasing the load-bearing capacity of compressed elements without increasing their weight (Goel et al., 2021). However, this leads to the production of increasingly slender elements that are prone to buckling. In the case of rods with significant imperfections (geometric, material), it is relatively difficult to determine the onset of instability and to identify the critical force. Therefore, for rods with a constant cross-section, the Southwell method is widely known and used to determine the value of the critical load (Rykaluk, 2012; Timoshenko & Gere, 1963).

The equilibrium paths of compressed structural elements exhibit a significant increase in force with minimal displacement growth, and then, near the critical force values, the graphs curve and change character (a very small force increase implies significant deformations). However, in the case of rods

[1] Corresponding author: University of Zielona Góra, Institute of Civil Engineering, Zielona Góra, Poland, e-mail: miroslaw.sadowski@gmail.com.

with significant geometric imperfections, this may not be noticeable. In other cases, the relative flattening of the equilibrium path cannot be observed in a form even remotely resembling the initial segment of the path. This makes the direct measurement of the critical force, by loading the rod until buckling occurs, difficult to achieve, if not impossible. In these circumstances, it is necessary to resort to another method to determine the critical force value. The Southwell method, based on measured values of the applied force and corresponding deflections, allows for determining the critical force value without the need to reach it during the experiment (Blostotsky et al., 2016; Mandal & Calladine, 2002; Valsangkar et al., 1981).

The Southwell method was derived assuming linear elastic material properties and a constant cross-section along the length of the compressed rod (Southwell, 1932). Attempts to modify the Southwell method occurred relatively quickly (Wang, 1948; Ariaratnam, 1961; Singer, 1989) and are still the subject of research today. In his work, Dinnik (1935) addresses, among other things, the eigenvalue problem for rods whose shape is defined by power functions up to the fourth degree. Ariaratnam highlighted the possibility of applying the method to compressed rods with different support conditions and rods with variable bending stiffness (Ariaratnam, 1961). The work of Bo-Hao et al. (2013) describes the stability of double steel tapered columns with a tubular cross-section. Marcinowski et al. (2020) discuss the optimization of the stability of non-prismatic rods using complex functions, while their subsequent work (2021) deals with the optimization of non-prismatic rods with variable wall thickness—both in the context of the Southwell method. In another work, Marcinowski et al. (2022) demonstrated that the method could also be successfully applied to rods with variable cross-sections and linear elastic material characteristics.

It should be emphasized that there are no standardized and easy-to-apply algorithms for studying the stability of such structural elements (Marques et al., 2012), and those that exist for specific cases are usually quite complex (Serna et al., 2011).

Further attempts to modify the Southwell method involve transferring it to physically nonlinear materials. This is due to the fact that most construction materials follow Hooke's linear law only within small deformations, and in many cases, the examined objects are operated under deformations exceeding the linear range (Krysko et al., 2021). Let's take a closer look at the conducted studies.

The mechanical response of a homogeneous, isotropic elastic material can be fully characterized by two physical constants, namely Young's modulus and Poisson's ratio. However, the physical reactions of nonlinear materials are described by parameters that are scalar functions of deformation, and their specific choice is not always clear (Mihai, Goriely, 2017).

The problem of studying the behavior of materials with different moduli has attracted the attention of many researchers. Birger proposed a modification of the elastic solution method, i.e., the variable stiffness method, to solve physically nonlinear problems in plasticity and creep theory (Birger, 1951). Bert's model is based on the criterion of positive and negative signs of longitudinal fiber deformations and is widely used in multilayer composites (Bert, 1977). Jones proposed a modified model for isotropic and orthotropic bimodular materials (Jones, 1977). Ambartsumian's bimodular model for isotropic materials assumes different tensile and compressive moduli based on positive and negative stress signs, which is particularly important in structural analysis and design (Ambartsumian, 1986). Chen et al. used Timoshenko beam theory to study the dynamic stability of a bimodular beam under periodic axial loading (Chen, 1991). Baykara et al. investigated the large deflection of a thin beam under the influence of an end moment, particularly analyzing the influence of a nonlinear bimodular material on horizontal and vertical deflection based on numerical simulations (Baykara, 2005). Shatnawi and Al-Sadder provided an exact solution for the large deflection of non-prismatic cantilever beams made of bimodular material (Shatnawi et al., 2007). Lü et al. obtained solutions for bending elasticity and thermal deformation of functionally graded beams with different end conditions, using the state space differential

quadrature method. The considered beams were macroscopically isotropic, and Young's modulus varied exponentially along the thickness and longitudinal direction (Lü et al., 2008). Pavilaynen's works presented the bending results of multimodular beams under concentrated or distributed loads. The standard Bernoulli-Euler beam hypotheses and Illyushin's plasticity theory were used (Pavilaynen, 2015). Awrejcewicz et al. (2017) presented a new mathematical model of elastic-plastic beams, rigidly fixed at the ends, under transverse pressure. The model considered moving elastic bending waves, stationary and non-stationary plastic hinges, elastic-plastic stretching, and shear deformation. Tran and Shapiro's work presented a nonlinear deformation analysis of prestressed beam systems used in road bridge spans or high-rise buildings using a nonlinear material model (Tran, Shapiro, 2019).

Building upon and developing this topic, the authors aimed to demonstrate that the Southwell method is equally effective for rods made of elastic materials with strongly nonlinear but elastic $\sigma(\varepsilon)$ characteristics.

The adopted procedure involved determining the relationship between the compressive force F and the deflection δ, i.e., the $F(\delta)$ characteristic, for a rod with a predefined small initial arc imperfection δ_0, and constructing Southwell plots based on this. The detailed considerations included strongly nonlinear characteristics and were conducted for a rod with a rectangular cross-section, predefined cross-sectional dimensions, assumed length, and pinned supports at both ends. The *Mathematica*™ program was used for analytical transformations. The presented considerations included both materials with identical $\sigma(\varepsilon)$ characteristics for compression and tension (symmetric material) and different characteristics for these two ranges (asymmetric material).

2. SUBJECT OF STUDY

The subject of detailed considerations is a compressed rod made of a material defined by relations (2.1) and (2.2) and meeting the basic assumption of the Euler-Bernoulli theory: bending deformations along the height of the cross-section change linearly and are proportional to the curvature of the bent rod. The modulus is variable, and for the current value of ε, it is defined by the differential relationship $d\sigma/d\varepsilon$.

The rod is pin-supported at its ends, and its static diagram is shown in Figure 1.

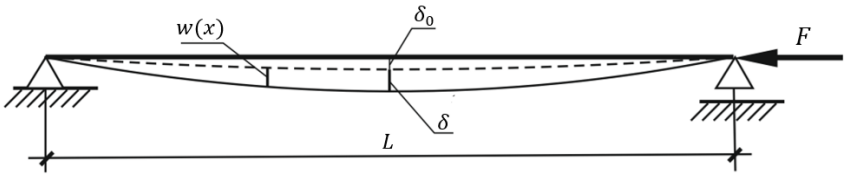

Fig. 1. Static diagram of the analyzed rod

The rod has a length L = 1000 mm and is characterized by a constant rectangular cross-section ($b \times h = 30 \times 10$ [mm]). At the same time, it is assumed that the rod is burdened with an initial arc imperfection, the amplitude of which has a value $\delta_0 = 0.5$ mm.

For detailed considerations, three hypothetical models of stress-strain characteristics $\sigma(\varepsilon)$, symmetrical for the compression zone and the tension zone, were adopted (Fig. 2):

$$\begin{aligned} \sigma_1(\varepsilon) &= 52.5\ \text{arsinh}\ (4000\varepsilon) \\ \sigma_2(\varepsilon) &= 150\ \text{arctg}\ (1400\varepsilon) \\ \sigma_3(\varepsilon) &= 250\ \text{tgh}\ (840\varepsilon) \end{aligned} \tag{2.1}$$

In the presented analyses, it is necessary to use the inverse of these functions in the form $\varepsilon(\sigma)$:

$$\begin{aligned} \varepsilon_1(\sigma) &= \frac{1}{4000}\ \text{sinh}\ \left(\frac{\sigma}{52.5}\right) \\ \varepsilon_2(\sigma) &= \frac{1}{1400}\ \text{tg}\ (150\sigma) \\ \varepsilon_3(\sigma) &= \frac{1}{840}\ \text{artgh}\ \left(\frac{\sigma}{250}\right) \end{aligned} \tag{2.2}$$

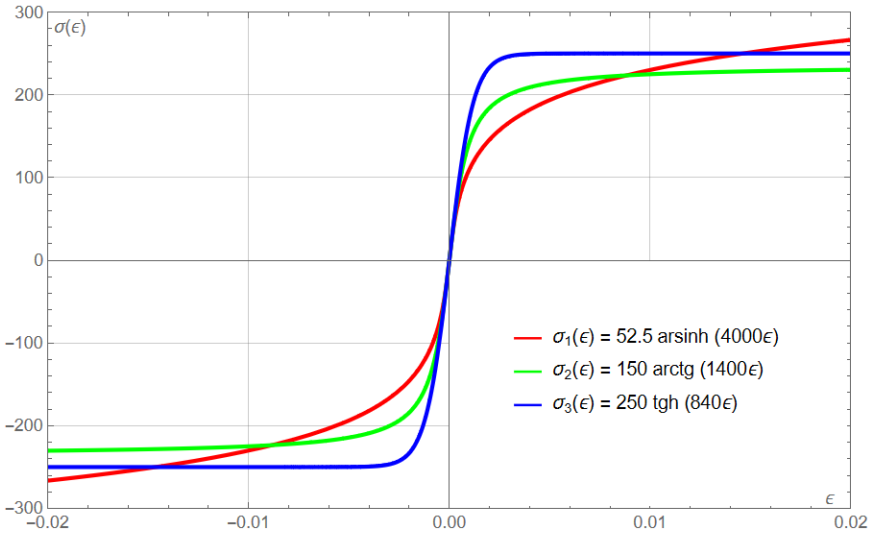

Fig. 2. Material characteristics adopted in (2.1)

One hypothetical stress-strain characteristic model $\sigma(\varepsilon)$, asymmetric for the compression zone and the tension zone, was also used in further considerations (Fig. 3):

$$\sigma(\varepsilon) = \begin{cases} \sigma_s(\varepsilon) = 350\ \text{arctg}\ (600\varepsilon), & \text{for} \quad \varepsilon < 0 \\ \sigma_r(\varepsilon) = 60\ \text{arsinh}(3500\varepsilon), & \text{for} \quad \varepsilon \geq 0 \end{cases} \tag{2.3}$$

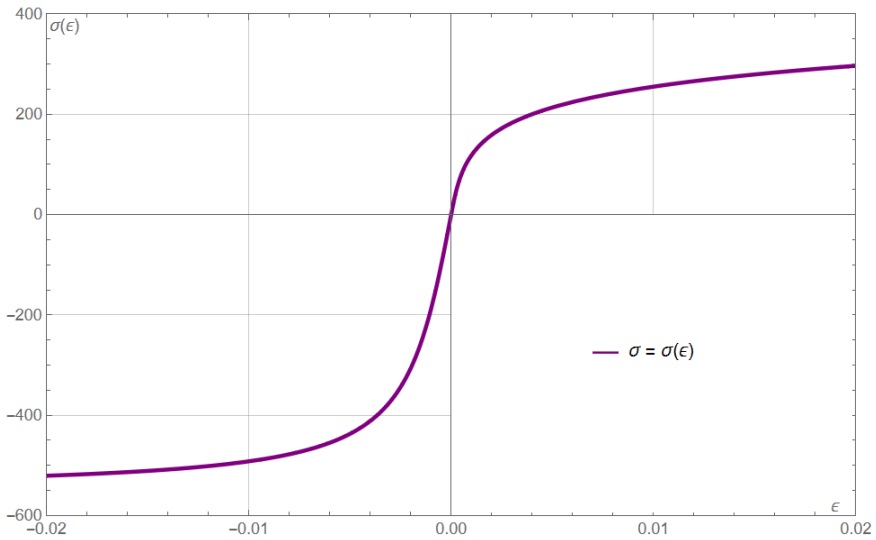

Fig. 3. Material characteristics (2.3)

Given the analysis being conducted, it is necessary to use the inverse of this function $\left(\varepsilon(\sigma)\right)$:

$$\varepsilon(\sigma) = \begin{cases} \varepsilon_s(\sigma) = \frac{1}{600}\,\mathrm{tg}\left(\frac{\sigma}{350}\right), & \text{for } \sigma < 0 \\ \varepsilon_r(\sigma) = \frac{1}{3500}\sinh\left(\frac{\sigma}{60}\right), & \text{for } \sigma \geq 0 \end{cases} \tag{2.4}$$

In the cases under consideration, it is not possible to use the differential equation of the deflection line of a compression bar to determine the value of the critical force, which, according to the classical theory of bar bending, presents the equation

$$EI\frac{1}{\varrho} = -M(x) \tag{2.5}$$

– it is necessary to resort to the theory of inelastic buckling of bars, according to which (cf. Timoshenko, Gere, 1963)

$$\int_A \sigma z dA = M. \tag{2.6}$$

3. MATHEMATICAL MODEL OF THE ADOPTED RESEARCH SUBJECT

The distributions of deformations and stresses in a bar subjected to pure compression and pure bending are shown in Figures 4 - 5. In the case of bending, the distribution of deformations results from the the assumption of preserving the flatness of the section: strains vary linearly as a function of the coordinate (z) measured from the neutral axis of the section. The magnitude ϱ is the local radius of curvature of the rod axis.

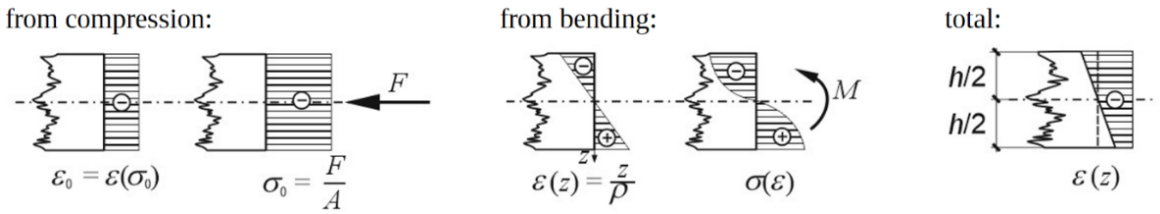

Fig. 4. Distribution of strains and stresses due to compression and bending
(rod with symmetrical characteristics $\sigma(\varepsilon)$)

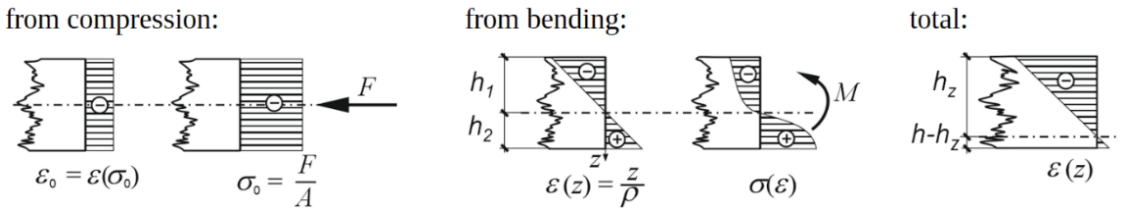

Fig. 5. Distribution of strains and stresses due to compression and bending
(rod with asymmetrical characteristics $\sigma(\varepsilon)$)

In a bar with an initial arc curvature, subjected to a compressive force, a complex state of stress (compression with bending) arises. Relation (2.6) written at the location of the maximum moment ($x = L/2$) takes the form:

$$\int_A \sigma\left(\frac{z}{\varrho} - \varepsilon_0\right) z\, dA = F(\delta + \delta_0), \tag{3.1}$$

where:
- ✓ $\sigma_0 = F/A$ – compressive stresses ($A = bh$),
- ✓ $\sigma(z/\varrho - \varepsilon_0)$ – bending stresses ($\varepsilon_0 = \varepsilon(F/A)$),
- ✓ ϱ – rod curvature,
- ✓ δ – the amplitude of rod deflection caused by force F,
- ✓ δ_0 – the amplitude of the initial arc imperfection (Fig. 1).

In the case of a rod with a symmetric stress-strain characteristics, relation (3.1) translates into the relation

$$\int_{-h/2}^{h/2} \sigma\left(\frac{z}{\varrho} - \varepsilon\left(\frac{F}{A}\right)\right) bz\, dz = F(\delta + \delta_0). \tag{3.2}$$

For a rod with an asymmetric stress-strain characteristics distribution, the relationship (3.1) adopts the form:

$$\int_{-h_1}^{h_z - h_1} \sigma_s\left(\frac{z}{\varrho} - \varepsilon_s\left(\frac{F}{A}\right)\right) bz\, dz + \int_{h_z - h_1}^{h - h_1} \sigma_r\left(\frac{z}{\varrho} - \varepsilon_r\left(\frac{F}{A}\right)\right) bz\, dz = F(\delta + \delta_0), \tag{3.3}$$

whereby (cf. Fig. 6)

$$h_z = \frac{|g|h}{d+|g|} \tag{3.4}$$

where

$$g = \frac{-h_1}{\varrho} - \varepsilon_s\left(\frac{F}{A}\right), \quad d = \frac{h-h_1}{\varrho} - \varepsilon_s\left(\frac{F}{A}\right) \tag{3.5}$$

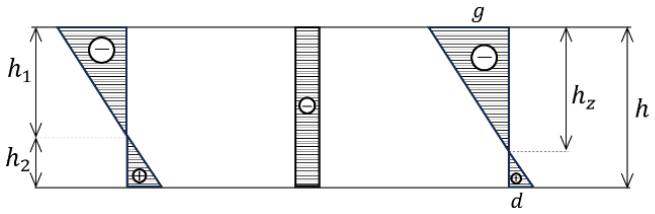

$$\varepsilon(z) = \frac{z}{\varrho} \qquad \varepsilon_0 = \varepsilon\left(\frac{F}{A}\right) \qquad \varepsilon(z) = \frac{z}{\varrho} - \varepsilon\left(\frac{F}{A}\right)$$

Fig 6. Strain distribution

Suppose that the deflection of the rod (Fig. 1) is determined by the relationship

$$w(x) = \delta \sin\frac{\pi}{L}x \tag{3.6}$$

and that these deflections have a relatively small value. In view of this, the curvature at the center of the bar length

$$\left|\frac{1}{\varrho}\right|_{x=L/2} \approx \left|\frac{d^2w}{dx^2}\right|_{x=L/2} = \left(\frac{\pi}{L}\right)^2 \delta, \tag{3.7}$$

hence

$$\varrho = \frac{L^2}{\pi^2\delta}. \tag{3.8}$$

Equations (3.2) and (3.3), due to the relationships determining stresses and strains, are transcendental equations, the solution of which poses some difficulties, however, they could be successfully solved using numerical programs (the Mathematica™ program was used for the purpose of this work), obtaining a sequence solutions for each model.
It was assumed that:

- ✓ the value of the amplitude of the initial arc imperfection: $\delta_0 = 0.5\ [mm]$,
- ✓ the value of the bar deflection amplitude caused by force F: $\delta = \{0.05 - 50\}\ [mm]$,
- ✓ the position of the neutral axis in the section of a rod with nonlinear non-symmetric material characteristics (h_1), corresponding to the deflection δ, is defined by the relation:

$$\int_A \sigma dA = 0, \tag{3.9}$$

which reduces to the form

$$-\int_{-h_1}^{0} \sigma_s\left(\frac{z}{\varrho}\right) dz = \int_0^{h-h_1} \sigma_r\left(\frac{z}{\varrho}\right) dz, \tag{3.10}$$

where σ_s i σ_r determine the relationships (2.4).

By solving the considered transcendental equations, the value of the corresponding force was obtained – in this way, equilibrium paths were built $F = F(\delta)$.

4. NUMERICAL ANALYSIS OF SELECTED CASES

4.1. Symmetric stress distribution models for the compression zone and the tension zone

The numerical analysis was carried out for each of the above-mentioned models (2.1), however, due to the qualitative repeatability of the obtained data, the results for one of them are presented below – defined by the relation $\sigma_1(\varepsilon) = 52.5 \operatorname{arsinh}(4000\varepsilon)$; a summary of the data for further models (2.1) are presented in tables below.

As a result of the calculations, a sequence of points (F, δ) was obtained, which is shown graphically in Fig. 7.

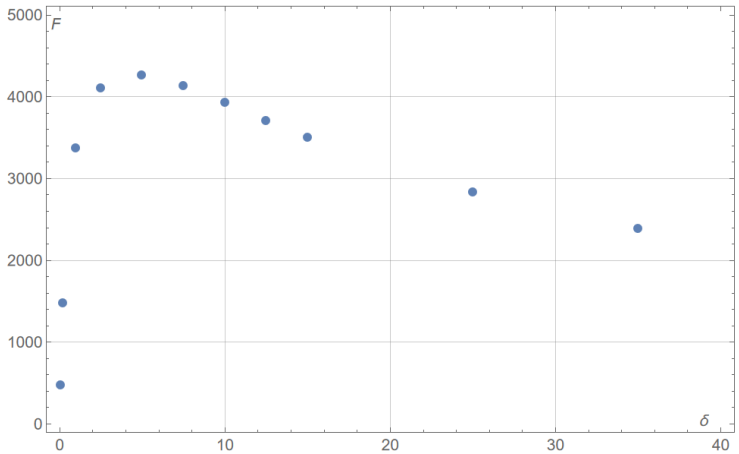

Fig. 7. Equilibrium path $F = F(\delta)$ – stress model *arsinh*

In the classical Southwell method, the initial part of the graph $F(\delta)$ is transformed to the form $\delta/F = \delta/F(\delta)$. This operation does not pose any major difficulties. Figure 8 shows the effect of transforming the initial section of the equilibrium path shown in Figure 7 into a Southwell straight line.

As can be seen, the linear nature of the relationship $\delta/F = \delta/F(\delta)$ is fully confirmed. The regression line for the above data is described by the equation

$$\frac{\delta}{F}(\delta) = 2.1538 \cdot 10^{-4}\delta + 8.74695 \cdot 10^{-5}. \tag{4.1}$$

The value of the critical force, which is the inverse of the directional coefficient of Southwell's straight line, is as follows: $F_{kr} = (2.1538 \cdot 10^{-4})^{-1} = 4642.96\ N$. The value of Pearson's linear correlation coefficient (R^2 = 0.999396) indicates a virtually complete positive linear relationship between the values obtained.

It should be emphasized that in the conducted studies, almost full positive linear correspondence between the obtained values was always obtained, i.e. the value of Pearson's linear correlation coefficient was located at the level of 0.99 and above, even close to 1.

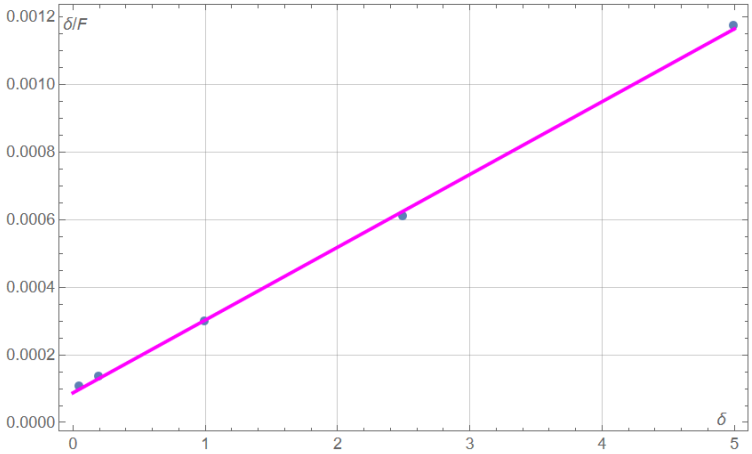

Fig. 8. Graphic equilibrium path of a compression rod in the relationship $\delta/F = f(\delta)$

Based on the analysis sequence, using Southwell's method, the critical forces and stresses shown in Table 1 for each model were obtained.

Table 1. Values of critical forces and critical stresses of individual stress models

stress model	critical force [N]	critical stress [MPa]
arsinh	4642.96	15.48
arctg	4753.61	15.85
tgh	4842.09	16.14

The analysis also yielded values of critical forces and corresponding critical stresses, knowledge of which makes it possible to determine $\varepsilon_{kr} = \varepsilon(\sigma_{kr})$ for each of the characteristics, as well as different variants of equivalent moduli, defined by the relations

✓ tangent module

$$E_{st} = \frac{d\sigma(\varepsilon_{kr})}{d\varepsilon} \tag{4.2}$$

✓ Engesser-Karman equivalent module (Lubinski et al., 1986 and Jakubowicz et al., 1978):

$$E_{E-K} = \frac{4EE_{st}}{\left(\sqrt{E}+\sqrt{E_{st}}\right)^2} \tag{4.3}$$

where $E = \frac{d\sigma(0)}{d\varepsilon}$, while E_{st} is defined by the relationship (4.2),

✓ alternative module[2]

$$E_{Alt} = \frac{(E_{st})^2}{E}. \tag{4.4}$$

Based on this, the value of the critical force could be calculated using a modified Euler's formula

$$F_{kr} = \frac{\pi^2 E^* J}{L^2}, \tag{4.5}$$

where $J = bh^3/12$ is the moment of inertia of the section, while E^* is the modulus defined according to the relations (4.2) – (4.4). The obtained values of moduli and critical forces are summarized in Table 2. The most authoritative value is that obtained by the Southwell procedure. Proposals for the use of equivalent moduli are better suited to the case of elastic-plastic materials.

Table 2. Summary of the values of critical forces of individual stress models, obtained by applying the Southwell method and the modified Euler's formula

stress model	critical force[3] [N]	module [MPa]		critical force [N]	difference in the values of critical force [%]
arsinh	4642.96 N	E_{st}	201 191	4 964.18	6.92
		E_{E-K}	205 525	5 071.11	9.22
		E_{Alt}	191 751	4 755.94	2.43

[2] The proposed relationship is a suggestion by the authors. There is no doubt that the relationship should be subjected to further research and verification, the purpose of which is to assess its usefulness in the case of general.

[3] Obtained by applying the Southwell method.

arctg	4753.61 N	E_{st}	207 530	5 120.60	4.73
		E_{E-K}	208 760	5 150.93	5.35
		E_{Alt}	205 089	5 060.37	3.50
tgh	4842.09 N	E_{st}	209 024	5 157.47	0.88
		E_{E-K}	209 511	5169.49	1.12
		E_{Alt}	208 053	5 133.51	0.41

It is worth emphasizing that the independent use of the modified Euler's formula is impossible in the case of nonlinear material. The force F_{kr} causing flexural buckling of the bar and required to determination of E_{st} can only be determined using the procedure presented above.

4.2. Asymmetric stress distribution model for compression zone and tension zone

In the analysis presented here, the model described by equations (2.3) and shown in Fig. 3 was used. From the solution of the transcendental equation (3.3), the value of the corresponding force was obtained – thus, the equilibrium path $F = F(\delta)$ was constructed (see Figure 9).

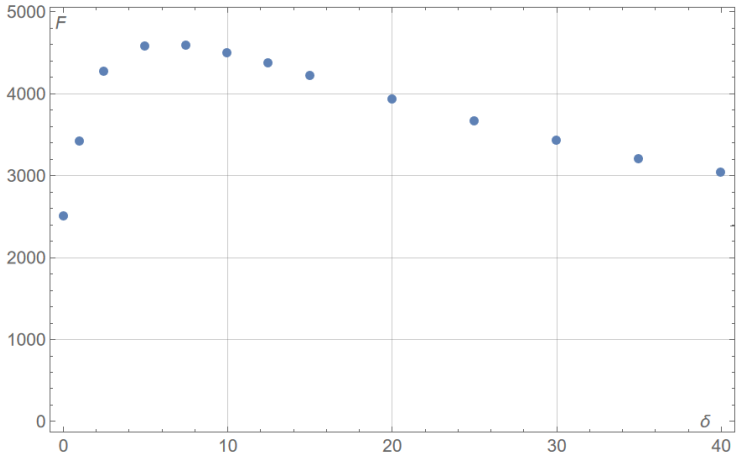

Fig. 9. The equilibrium path $F = F(\delta)$

Again, the effect of transforming the initial portion of the equilibrium path shown in Figure 9 into a Southwell straight line is shown, cf. Fig. 10.

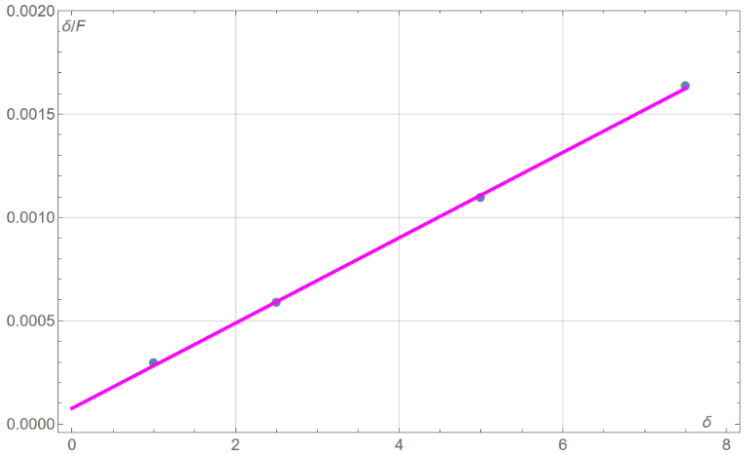

Fig. 10. Graphic equilibrium path of a compression rod in the relationship $\delta/F = f(\delta)$

Figure 10 fully confirms the linear nature of the Southwell curve. The regression line for the above data is described by the equation

$$\frac{\delta}{F}(\delta) = 2.06525 \cdot 10^{-4}\delta + 7.54175 \cdot 10^{-5}. \tag{4.6}$$

The value of the critical force, which is the inverse of the directional coefficient of Southwell's straight line, is as follows: $F_{kr} = (2.06525 \cdot 10^{-4})^{-1} = 4842.03\ N$. The value of Pearson's linear correlation coefficient (R^2 = 0.999504), indicates practically a full positive linear relationship between the obtained values.

The value of critical force and critical stress are shown in Table 3.

Table 3. Values of critical forces and critical stresses for the asymmetric stress model

stress model	critical force [N]	critical stress [MPa]
asymmetric	4 842.03	16.14

As before, knowledge of the critical stresses given in Table 3 makes it possible to determine $\varepsilon_{kr} = \varepsilon(\sigma_{kr})$ and the values of other moduli (cf. (4.2) – (4.4)). On this basis, the value of the critical force could be calculated from the modified Euler's formula (4.5).

The obtained critical force values are summarized in Table 4.

Table 4. Summary of the critical force values,
obtained by applying the Southwell method and the modified Euler's formula

stress model	critical force[4] [N]	module value [MPa]		critical force from Euler's formula [N]	difference in the values of critical forces [%]
asymmetric	4 842.03	E_{st}	202 625	4 999.56	3.25
		E_{E-K}	206 263	5 089.33	5.11
		E_{Alt}	195 508	4 823.97	0.37

5. NUMERICAL ANALYSIS

Equilibrium paths $F(\delta)$ determined analytically for the considered cases of material characteristics, were also determined numerically using the COSMOS/M program based on the finite element method. The bar shown shown in Figure 1 was replaced by a discrete model consisting of 100 finite elements of the BEAM2D type (cf. Rusinski, 1994), each 10 mm long. For comparative analyses, a symmetric model $\sigma_1(\varepsilon) = 52.5 \operatorname{arsinh}(4000\varepsilon)$ was selected from model group (2.1) and an asymmetric model defined by formulas (2.3).

Among the various material models implemented in COSMOS/M are elastic models with a nonlinear characteristic loaded as a point relation $\sigma(\varepsilon)$. This relationship is loaded as the so-called material curve.

Equilibrium paths were determined by geometrically nonlinear analysis; large displacements and nonlinear geometric relationships adapted to such a range of displacements. The incrementally iterative method (Netwon – Raphson) with control of the transverse displacement of the center point and automatic correction of the calculation step was used.

Figure 11 shows a comparison of equilibrium paths obtained by the analytical method and the numerical method for the chosen symmetric material model.

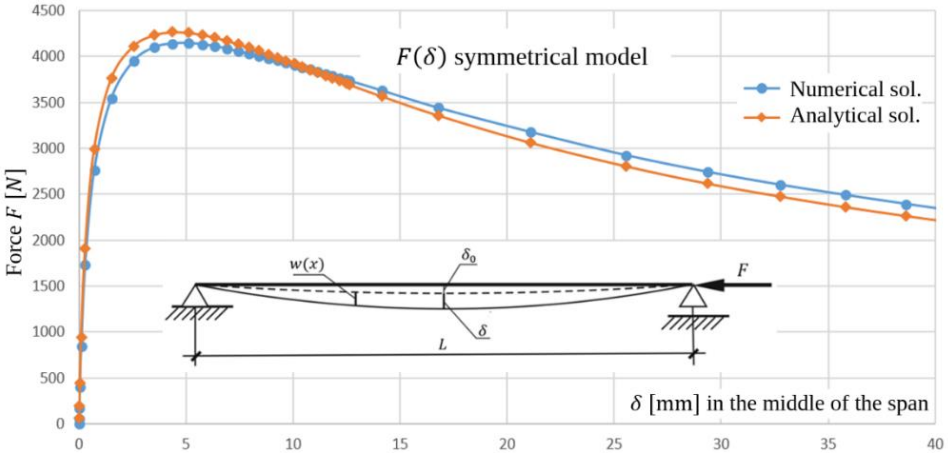

Fig. 11. Comparison of nonlinear equilibrium paths for symmetric material model

[4] Obtained by applying the Southwell method.

Figure 12 shows a comparison of the equilibrium paths obtained by the analytical method and the numerical method for an asymmetric material model.

Numerical simulations confirmed the correctness of equilibrium paths determination by the proposed analytical methods. The differences noted in Figures 11 and 12 are small and are due to the linear approximation of curvature as a function of rod deflection.

Southwell's method uses successive equilibrium path points from the range preceding the extremum. In this range, the agreement of the numerical solution with the analytical solution is even better, and therefore, the correctness of the procedure used to determine the critical load is not in doubt.

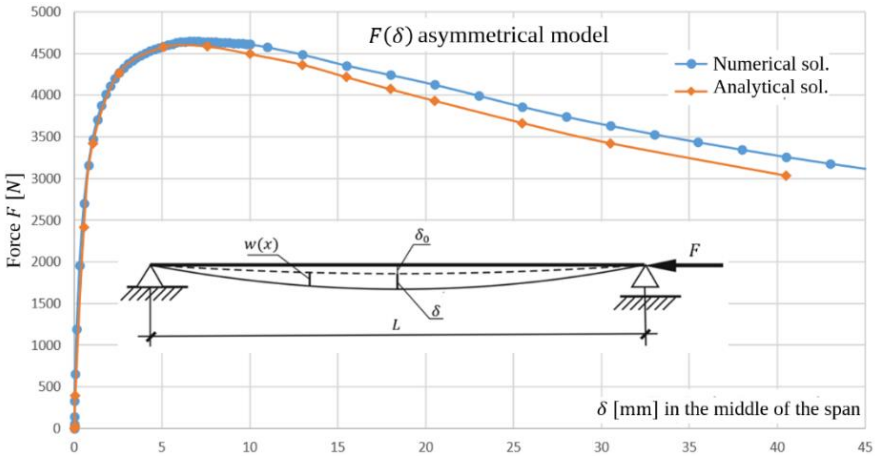

Fig. 12. Comparison of nonlinear equilibrium paths for asymmetric material model

6. RECAPITULATION

Thanks to developments in mechanics and materials and composites, the strength of compression members has been greatly increased, without a significant increase in "their size", which in turn results in very slender components susceptible to global or localized loss of stability. Heterogeneity in compression members can be achieved in two ways – by varying material properties or by changing the shape and cross-section. Both methods have advantages because the corollary of their use is a reduction in dead weight (Goel et al., 2021).

As mentioned at the beginning, the study of the behavior of compression rods shows that the equilibrium path of these members in its initial range shows a significant increase in force, with a simultaneous negligible increase in displacement, and then, at values close to the critical force, the graph curves and changes character - a very small increase in force implies significant lateral deformations (Marcinowski, 2017). This makes direct measurement of the critical force, realized by loading the bar, up to the occurrence of buckling is difficult to implement, if not impossible (Sadowski, 2018) or achievable only by numerical methods (Balduzzi et al., 2017), and particularly unpredictable in the case of elements exhibiting material nonlinearity. Under these circumstances, it is necessary to reach for another method to determine the value of the critical force. This is successfully accomplished by the method presented in the work. It consists of the first stage, in which a sequence of points is determined on a nonlinear equilibrium path by means of solving a transcendental equation, and the second stage, in which the critical force is obtained using the classical Southwell method.

Southwell's method correct for prismatic rods of constant (Ariaratnam, 1961) and variable cross-section (Marcinowski et al., 2022), made of materials exhibiting linear elasticity is also correct for compressed prismatic rods made of materials exhibiting elastic nonlinearity. The examples presented in the paper confirm this throughout.

According to the authors, the conducted research has led to the conclusion that the thesis formulated as follows – *Southwell's method is fit for studying the behavior of compression rods made of physically nonlinear, elastic material* is true.

REFERENCES

1. Ambartsumyan, SA 1986. Elasticity Theory of Different Moduli. *China Railway Publishing House*, Beijing.
2. Ariaratnam, ST 1961. The Southwell Method for Predicting Critical Loads of Elastic Structures, *Quart. J. Mech. and Appl. Math*., **14,** 137-153.
3. Awrejcewicz, J, Krysko, VA, Sopenko, AA, Zhigalov, MV, Kirichenko, AV, Krysko, AV 2017. Mathematical modelling of physically/geometrically non-linear micro-shells with account of coupling of temperature and deformation fields. Chaos Solit. Fract. **104**, 635–654. https://doi.org/10.1016/j.chaos.2017.09.008.
4. Balduzzi, G, Morganti, S, Auricchio, F and Reali, A 2017. Non-prismatic Timoshenko-like beam model: Numerical solution via isogeometric collocation. *Computers and Mathematics with Applications* **74** 1531–1541.
5. Baykara, C, Guven, U and Bayer, I 2005. Large deflections of a cantilever beam of nonlinear bimodulus material subjected to an end moment. *Int. J. Eng. Sci.* **24**(12), 1321–1326. https://doi.org/10.1177/0731684405049857.
6. Bert, CW 1977. Models for fibrous composites with different properties in tension and compression. *ASME J. Eng. Mater. Technol*. **99**, 344–349. https://doi.org/10.1115/1.3443550.
7. Birger, A 1951. Some general methods of solution for problems in the theory of plasticity. *Prikl. Mat. Mekh*. **25**(6).
8. Blostotsky, B, Efraim, E, Stanevsky, O, Kucherov, L and Zakrassov, A 2016. Extended options and improved accuracy for determining of buckling load with Southwell plot method. The Ninth International Conference on Material Technologies and Modeling MMT-2016.
9. Bo-Hao, Z, Yan-Lin, G and Chao, D 2013. Ultimate bearing capacity of asymmetrically double tapered steel columns with tubular cross-section, *Journal of Constructional Steel Research* **89** 52–62.
10. Chen, LY, Lin PD, Chen LW 1991. Dynamic stability of thick bimodulus beam. Comput. Struct. **41**(2), 257–263. https://doi.org/10.1016/0045-7949(91)90429-P.
11. Dinnik, AN 1935. Stability of elastic systems, NTI NKTP USSR, Moscow, Leningrad.
12. Goel, M, Bedon, Ch, Singh, A, Khatri, A and Gupta, L 2021. An Abridged Review of Buckling Analysis of Compression Members in Construction. Buildings 2021, 11, 211. https://doi.org/10.3390/buildings11050211.
13. Jakubowicz, A, Orłoś, Z 1978. Strength of materials. Scientific and Technical Publishing House, Warsaw.
14. Jones, RM 1977: Stress-strain relations for materials with different moduli in tension and compression. *AIAA J*. **15**(1), 16–23. https://doi.org/10.2514/3.7297.

15. Krysko, AV, Awrejcewicz, J, Bodyagina, KS and Zhigalov, MV 2021. Mathematical modeling of physically nonlinear 3D beams and plates made of multimodulus materials. *Acta Mech* **232**, 3441–3469 (https://doi.org/10.1007/s00707-021-03010-8).
16. Lü, CF, Chen, WQ, Xu, RQ, Lim, CW 2008. Semi-analyical elasticity solutions for bi-directional functionally graded beams. *Int. J. Sol. Struct*. **45**, 258–275.. https://doi.org/10.1016/j.ijsolstr.2007.07.018.
17. Łubiński, M, Filipowicz, A, Żółtowski, W 1986. Metal structures. Part I. Fundamentals of design. Arkady Publishing House, Warsaw.
18. Mandal, P, Calladine, CR 2002. Lateral-torsional buckling of beams and the Southwell plot. *International Journal of Mechanical Sciences*, Prof Publishing, **44** (12) 2557-2571.
19. Marcinowski, J 2017. Stability of elastic structures. Bar structures, arches, shells. Lower Silesian Educational Publishing House, Wrocław.
20. Marcinowski, J and Sadowski, M 2021. Designing of steel chs columns showing maximum compression resistance. *Civil And Env. Eng.Reports CEER*; **31** (1): 0079-0092.
21. Marcinowski, J and Sadowski, M 2020. Using the erfi function in the problem of the shape optimization of the compressed rod. *Int. J. of Applied Mechanics and Engineering*, vol. **25**, No.2, pp.75-87.
22. Marcinowski, J, Sadowski, M and Sakharov, V 2022. On the applicability of Southwell's method to the determination of the critical force of elastic columns of variable cross sections. *Acta Mech* **233**, 4861–4875 (https://doi.org/10.1007/s00707-022-03345-w).
23. Marques, L, Taras, A, da Silva, LS and Rebelo, C 2012. Development of a consistent buckling design procedure for tapered columns. *Journal of Constructional Steel Research* **72** 61–74.
24. Mihai, A, Goriely, A 2017. How to characterize anonlinear elastic material? A review on nonlinear constitutive parameters inisotropic finite elasticity. rspa.royalsocietypublishing.org (http://dx.doi.org/10.1098/rspa.2017.0607).
25. Pavilaynen, G 2015. Elastic-plastic deformations of a beam with the SD-effect. AIP Conf. Proc. **1648**, 300007. https://doi.org/10.1063/1.4912549.
26. Pavilaynen, GV 2015. Mathematical model for the bending of plastically anisotropic beams. Vest. St. Petersburg Univ. Math. **48**, 275–279.
27. Rusiński, E 1994. Finite element method: the COSMOS/M system, Publishing House of Communications, Warsaw.
28. Rykaluk, K 2012. Issues on stability of metal structures. Lower Silesian Educational Publishing House, Wrocław.
29. Sadowski, M 2018. Spatial shaping of bars compressed with maximum buckling capacity. Doctoral dissertation, Zielona Góra.
30. Serna, MA, Ibáñez, JR and López, A 2011. Elastic flexural buckling of non-uniform members: Closed-form expression and equivalent load approach. *Journal of Constructional Steel Research* **67** 1078–1085.
31. Shatnawi, AS and Al-Sadder, S 2007. Exact large deflection analysis of nonprismatic cantilever beams of nonlinear bimodulus material subjected to tip moment. *J. Reinf. Plast. Compos*. **26**(12), 1253–1258. https://doi.org/10.1177/0731684407079754.
32. Singer, J 1989. On the Applicability of the Southwell Plot to Plastic Buckling. *Experimental Mechanics*, **29**(2), 205-208.
33. Southwell, RV 1932, On the analysis of experimental observations in problems of elastic stability. *Proc Royal Soc*, Ser A **135**, pp. 601-616.
34. Timoshenko, S and Gere, JM 1963. Theory of Elastic Stability. McGraw Hill Book Company, Inc., 2nd Ed.

35. Valsangkar, AJ, Britto, AM and Gunn, MJ 1981. Application of the Southwell plot method to the inspection and testing of buried flexible pipes. *Proc. Instn Ciu. Engrs, Part* **2**,1982,73, 217-221.
36. Van Tran, TT and Shapiro, D 2019. Nonlinear deformation analysis for precastpre-stressed concrete beam systems. FORM-2019 Web Conf. 97, 03039.
37. Wang, CT 1948. Inelastic Column Theories and an Analysis of Experimental Observations, *J. Aero. Sci*., **15**, 283-292.